

Published in final edited form as:

*Nat Geosci.* 2019 July 02; 12(9): 779–782. doi:10.1038/s41561-019-0414-7.

## Selenium isotopes as tracers of a late volatile contribution to Earth from the outer Solar System

María Isabel Varas-Reus<sup>1,\*</sup>, Stephan König<sup>1</sup>, Aierken Yierpan<sup>1</sup>, Jean-Pierre Lorand<sup>2</sup>, Ronny Schoenberg<sup>1</sup>

<sup>1</sup>Isotope Geochemistry, Department of Geosciences, University of Tuebingen, Tuebingen, Germany

<sup>2</sup>Laboratoire de Planétologie et Géodynamique à Nantes, CNRS UMR 6112, Université de Nantes, Nantes, France

### Abstract

The origin of Earth's volatiles has been attributed to a late addition of meteoritic material after core-mantle differentiation. The nature and consequences of this 'late veneer' are debated, but may be traced by isotopes of the highly siderophile, or iron-loving, and volatile element selenium. Here we present high-precision selenium isotope data for mantle peridotites, from double spike and hydride generation multi-collector inductively coupled plasma mass spectrometry. These data indicate that the selenium isotopic composition of peridotites is unaffected by petrological processes, such as melt depletion and melt-rock reaction, and thus a narrow range is preserved that is representative of the silicate Earth. We show that selenium isotopes record a signature of late accretion after core formation and that this signature overlaps only with that of the CI-type carbonaceous chondrites. We conclude that these isotopic constraints indicate the late veneer originated from the outer Solar System and was of lower mass than previously estimated. Thus, we suggest a late and highly concentrated delivery of volatiles enabled Earth to become habitable.

---

Volatiles are key in the development of Earth into a habitable planet, but their origin remains highly debated<sup>1–5</sup>. A 'late veneer' of chondrite-like material added to the bulk silicate Earth (BSE) after core formation had ceased, has been argued to be the most plausible source of Earth's volatiles<sup>4,5</sup>. This late veneer was originally proposed to account for the abundances of highly siderophile elements (HSEs) in the Earth's mantle<sup>6–8</sup>. The model was then extended to volatiles S, Se and Te<sup>5,6</sup>, as all these elements display broadly chondritic relative and absolute abundances in the Earth's mantle higher than experimentally predicted from metal/silicate partition coefficients and core-mantle differentiation models<sup>9–11</sup>. Despite the

---

Users may view, print, copy, and download text and data-mine the content in such documents, for the purposes of academic research, subject always to the full Conditions of use:[http://www.nature.com/authors/editorial\\_policies/license.html#terms](http://www.nature.com/authors/editorial_policies/license.html#terms)

\*Correspondence to: m.varas-reus@uni-tuebingen.de.

**Author Contributions:** S.K designed the project, J.P.L. provided the samples and their relevant petrogenetic features, M.I.V.-R. prepared the samples and performed the Se isotope analysis, and together with S.K. and A.Y. interpreted data and wrote the manuscript with contribution from all authors.

**Competing interests:** Authors declare no competing interests.

**Data availability.** The data that support the findings of this study are provided as Supplementary Tables 1-7.

potential role of the late veneer in Earth's volatile evolution<sup>3–5</sup>, its nature remains controversial. Based on Re-Os isotope systematics the late veneer composition was similar to that of ordinary or enstatite chondrites<sup>12,13</sup>, whereas the distinct nucleosynthetic Ru isotope anomalies between the Earth's mantle and known chondrites rule out an outer Solar System origin for the late veneer<sup>2</sup>. These isotope constraints discard carbonaceous chondrites, which based on their distinct isotope anomalies are considered to have formed in the outer Solar System<sup>14,15</sup>, as the source material of the late veneer. In contrast, the broadly chondritic S, Se and Te ratios in fertile peridotites suggest that the late veneer was volatile-rich and consisted mostly of carbonaceous chondrite-like materials<sup>5</sup>. However, the use of S, Se and Te ratios in mantle peridotites to trace the composition of the late veneer has been significantly weakened as their relative abundances may not represent a primitive feature of the BSE<sup>16,17</sup>.

Unraveling the link between the late veneer and Earth's volatiles has proved challenging mainly due to difficulties to establish precise and accurate volatile isotopic and compositional signatures in the BSE and to attribute them to a clear post-planetary core formation origin<sup>1,5,18</sup>. Here we use Se stable isotopes that, due to their unique properties, can clearly overcome these limitations. Se and Te are both volatile and behave like HSEs at core formation conditions<sup>9</sup>, and as HSEs they were almost entirely scavenged from the mantle during core segregation. This Se-Te depleted mantle provides an ideal background for the late veneer to leave a diagnostic signature of these elements. In addition, a recent high-precision study reported distinguishable Se isotope compositions between different classes of chondrites<sup>19</sup>. Altogether, this shows that Se isotopes may potentially be a strong diagnostic tool to identify the type of chondrite representative of the late veneer composition that left its mark in the BSE, provided that such a BSE signature can be established. However, a Se isotope composition of the BSE with similar high-precision to that of chondrites<sup>19</sup> is still missing. We here address this issue by investigating, for the first time, the Se isotope composition of mantle peridotites with a high-precision analytical technique.

## Se isotope signature of the BSE inferred from peridotites

For this study, we selected a set of representative mantle peridotites that range in age from Mid-Proterozoic to late Paleozoic and are from different geological settings and localities, including nine samples from orogenic and transitional peridotite massifs (Ronda, Pyrenees, Lanzo and External Ligurides) and two xenoliths from the French Massif Central (Supplementary Table 1). Samples were analysed for Se isotopes on a multi-collector inductively coupled plasma mass spectrometer (MC-ICP-MS) at the University of Tuebingen (Germany) using a double spike and methane-boosted hydride generation technique<sup>20,21</sup> (see Methods). Data are reported in  $\delta^{82/76}\text{Se}$  notation (Supplementary table 2), that is, the per mil (‰) variation of  $^{82}\text{Se}/^{76}\text{Se}$  relative to the reference material NIST SRM 3149.

The selected samples range from a refractory harzburgite ( $\text{Al}_2\text{O}_3$  ~0.7 wt.%; Se ~6 ng g<sup>-1</sup>) to a highly fertile lherzolite ( $\text{Al}_2\text{O}_3$  ~4.2 wt.%; Se ~100 ng g<sup>-1</sup>). This sample set displays an apparently positive correlation between  $\text{Al}_2\text{O}_3$  and Se contents and encompasses the entire spectrum reported in the literature for peridotites in the  $\text{Al}_2\text{O}_3$  vs. Se space (Fig. 1a). Both

depletion and metasomatic re-enrichment processes can account for trends between  $\text{Al}_2\text{O}_3$  and Se concentrations in peridotites, and even refertilization and overprint of HSEs, including Se and Te, of originally refractory protoliths, have been reported<sup>16,22–25</sup>. However, regardless of these complex mantle processes that might have affected the Se budget of mantle peridotites, they do not produce a Se isotopic variation in peridotites, as shown by their homogeneous  $\delta^{82/76}\text{Se}$  values (Supplementary table 2) that have a mean of  $-0.03 \pm 0.07\text{‰}$  (2 s.d. of the mean,  $n=11$ ; Fig. 1b, c), and the lack of any correlation with petrogenetic indicators of melt depletion/metasomatism such as  $\text{Al}_2\text{O}_3$  (Fig. 1b) or Pd/Ir ratios (Supplementary Information). This is the most limited Se isotope range ever reported for a suite of mantle rocks of different ages and different geological settings, and it is independent of their Se content (Fig. 1c). Compared to peridotites, basaltic lavas from worldwide locations have heavier Se isotope values ( $0.23 \pm 0.14\text{‰}$ , 2 s.d. of the mean;  $n=4$ ; Fig. 2)<sup>20</sup>, whereas Pacific-Antarctic ridge MORBs are much lighter ( $-0.16 \pm 0.13\text{‰}$ , 2 s.d. of the mean;  $n=27$ ; Fig. 2)<sup>17</sup>. This Se isotope variability among basaltic melts might reflect additional processes<sup>26</sup>, emphasizing that selected peridotites, with their range of ages, may indeed represent the most robust estimate of the BSE Se isotope signature.

### Implications for the nature of the late veneer

The proposed average BSE Se isotope composition ( $-0.03 \pm 0.07\text{‰}$ , 2 s.d. of the mean) has a remarkably narrow range compared to previous estimates ( $0.33 \pm 0.32\text{‰}$ ; 2 s.d. analytical precision;  $n=10$ ; Fig. 2)<sup>27</sup>. This allows to resolve, for the first time, a Se isotopic variability between the BSE and different classes of chondrites (reported with 2 s.d. of the mean obtained following replicate measurements;  $n$ = number of chondrite subtypes analysed; Fig. 2)<sup>19</sup>. The significantly lighter and homogeneous  $\delta^{82/76}\text{Se}$  value of enstatite chondrites ( $-0.40 \pm 0.08\text{‰}$ ,  $n=3$ ) compared to that of the BSE discard these meteorites as the source of the Se isotopic signature of the BSE (Fig. 2). Ordinary chondrites ( $-0.21 \pm 0.10\text{‰}$ ,  $n=9$ ) and CO ( $-0.20 \pm 0.07\text{‰}$ ,  $n=2$ ) and CV ( $-0.24 \pm 0.10\text{‰}$ ,  $n=2$ ) carbonaceous chondrites can also be discarded as their mean  $\delta^{82/76}\text{Se}$  values are indistinguishable from each other<sup>19</sup> but are statistically significantly different than that of the BSE (Student's t-test, two-tail P-value  $< 0.0001$ ; Fig. 2). CM carbonaceous chondrites Murchison ( $0.20 \pm 0.13\text{‰}$ ) and Mighei ( $-0.30 \pm 0.10\text{‰}$ ) have substantial different positive and negative  $\delta^{82/76}\text{Se}$  values, respectively, plotting on both sides of the BSE (Fig. 2). These distinct  $\delta^{82/76}\text{Se}$  values suggest that a mixture of these two chondrites could result in a Se isotope signature that overlaps with that of the BSE. However, the possible proportional contributions of Mighei and Murchison chondrite-like material fall within a limited range ( $f = 0.69 \pm 0.2$ ;  $f$  denotes the proportion of source 1 in the mixture; Supplementary Information). Although CM chondrites cannot be refuted as the source of Se in the BSE, and other potential mixtures that involved CI chondrite-like material as the main source could be envisaged, the remarkable overlap of exclusively CI carbonaceous chondrites (mean  $\delta^{82/76}\text{Se}$  value of  $-0.02 \pm 0.12\text{‰}$ ,  $n=2$ ) with the BSE (Fig. 2) advocates for a simpler and straightforward scenario, where CI chondrites alone can account for the BSE Se isotope composition.

We conclude, based on the highly siderophile behavior of Se at core forming conditions and core-mantle differentiation that left the mantle almost completely devoid of Se<sup>9</sup>, that the main and most likely source of Se in the BSE was a CI chondrite-like late veneer. This

finding has striking implications for the mass of the late veneer and the amount of volatiles delivered by it. CI chondrites have the highest concentrations of volatiles among carbonaceous chondrites<sup>28</sup>, implying that compared to previous estimates calculated based on bulk chondritic composition<sup>8</sup> the mass of the late veneer would be lower. Unlike the estimated BSE Se-Te abundances that are controversial<sup>5,16,17</sup>, the S budget is known to retain an imprint acquired during core segregation<sup>29</sup> and thus it has been well constrained in the mantle before and after the late veneer<sup>30,31</sup>. Following a simple batch mixing calculation that assumes ~40% of S is in the pre-late veneer mantle<sup>30</sup> and a BSE S content of  $200 \pm 40 \mu\text{g g}^{-1}$ <sup>31</sup>, our mass balance calculations indicate that the total added material to the BSE by a CI chondrite-like late veneer would have been  $\sim 0.15 \pm 0.03\%$  of the Earth's mass (Supplementary Information). This estimate is significantly lower than  $\sim 0.5\%$  calculated based on mantle HSE abundances and a late veneer of bulk chondritic material<sup>8</sup>. Even considering a CM chondrite-like late veneer ( $\sim 0.26 \pm 0.05\%$  of the Earth's mass, Supplementary Information), the estimated mass would remain lower. This dichotomy could be reconciled if HSE partition coefficients during mantle-core differentiation conditions are lower than those previously reported<sup>10</sup>, as proposed for some HSEs<sup>10,11,32</sup>. Other more complex scenarios involving mixtures of CI chondrite-like material with a minor proportion of other carbonaceous or even ordinary chondrites could account for a Se isotope signature similar to that of the BSE. However, any of these potential mixtures will require more than 85% of CI chondrite-like material, with a similarly low-mass late veneer (Supplementary Information). Alternatively, it has been suggested that the late veneer involved a mixture of  $\sim 80\%$  carbonaceous chondrite-like material with  $\sim 20\%$  of a chemically evolved metal component derived from the core of a planetary embryo, similar in composition to iron meteorites<sup>33</sup>. Recent Ru isotopic data, however, have challenged this scenario and preclude that a chemically evolved metal component contributed significantly to the late veneer<sup>2,34</sup>. Independent of the likelihood of such intricate scenarios, the Se isotope approach clearly indicates that carbonaceous chondrites dominated the volatile late-accreted material.

These new Se isotope data are also at odds with the Re-Os isotope systematics that support an enstatite- or ordinary-chondrite-like late veneer<sup>12,13</sup> and with Ru isotope anomalies that infer an inner solar system origin for the late veneer<sup>2</sup>. The mass-dependent Ru isotope systematics, on the other hand, show no resolvable differences between the BSE and chondrites<sup>34</sup>, similar to the information conveyed by Pt and Pd stable isotopes<sup>35,36</sup>, and thus mass-dependent Ru isotope systematics cannot constrain which type of chondrite-like material dominated the late veneer. Furthermore, studies regarding the potential Ru isotope anomalies in the pre-late veneer mantle are currently underway to further assess the timing of volatile element accretion<sup>37</sup>. Regarding Os isotopes, Meisel et al.<sup>13</sup> and more recently Day et al.<sup>38</sup> reported indistinguishable  $^{187}\text{Os}/^{188}\text{Os}$  ratios for the BSE by extrapolating the correlations between a melt depletion indicator ( $\text{Al}_2\text{O}_3$ ) and the  $^{187}\text{Os}/^{188}\text{Os}$  ratios from worldwide peridotites. Their estimated BSE values (at 4 – 4.5 wt.%  $\text{Al}_2\text{O}_3$ ) are most similar to the average of ordinary and enstatite chondrites but are higher than those of carbonaceous chondrites<sup>13,38</sup> and any potential mixture that involves a large contribution from the latter (Supplementary Information). The Os isotopic composition of the BSE<sup>13,38</sup> could be reconciled with a late veneer composed of a mixture of carbonaceous chondrites with a chemically evolved metal component, as previously suggested<sup>33</sup>. However, as stated above,

this scenario is not supported by mass-dependent and –independent Ru isotopic data<sup>2,34</sup>. In any case, the narrow range of the BSE Se isotope signature reported here clearly overlaps only with that of CI chondrites (Fig. 2). Hence, this is unambiguous evidence that at least for volatiles, the late veneer comprised objects sourced from the outer solar system.

## Late volatile contribution from the outer Solar System

Considering a CI chondrite-like late veneer, and 40% S content in the pre-late veneer mantle<sup>30</sup>, the Se content of the BSE ( $47 \pm 10 \text{ ng g}^{-1}$ ; based on the new estimated late veneer mass, Supplementary Information) would have been delivered along with other volatiles<sup>4,5</sup>, but to a different extent. For S it is known that due to its moderately siderophile nature ~60% of the total S in the BSE was delivered after core formation<sup>30</sup>. Similar to Se, the highly siderophile behavior of Te during mantle-core differentiation supports a late veneer as its main source<sup>5,9</sup>, and yields a Te BSE abundance of  $5 \pm 1 \text{ ng g}^{-1}$  (Supplementary Information). This heterogeneous contribution of volatiles can also be extended to essential components for life such as water, carbon and nitrogen. On the basis of recent estimates of their BSE values, a CI chondrite-like late veneer would have delivered ~20-60% of water, from ~50% to even more than 120% of carbon, and an excess of nitrogen to the BSE. These estimates remain fairly similar if we consider a CM chondrite-like late veneer, as these chondrites are also volatile-rich materials, and would yield Se and Te abundances closer to those of highly fertile Iherzolites<sup>5,16,22</sup> (Supplementary Information). Our results imply that a percentage of water and probably carbon must have been delivered during the main stages of planetary accretion, in agreement with previous studies<sup>1,3,39,40</sup>. The excess abundance of nitrogen can be reconciled with considerable atmospheric loss<sup>41</sup> after the late veneer. Yet overall, although the proportion of volatiles delivered depend on their background mantle concentrations, our data also indicate that the late veneer contributed significantly to the Earth's volatile budget.

## Methods

Most of the samples analysed in this work were received as fine powder materials, except for sample 15-EDL/007, which was cut by a rock saw into smaller pieces that were then crushed and finally pulverised using an agate disc mill. Analytical procedures are described in detail in<sup>20,21</sup>, and only a brief summary of the most important aspects is given here.

Between 100 to 500 mg of sample powders were weighed in perfluoroalkoxy alkane beakers together with proportional amounts of <sup>77</sup>Se-<sup>74</sup>Se double spike solutions in order to ensure sample-spike equilibration during digestion. Samples were then digested following the hotplate HF-HNO<sub>3</sub> routine procedure described in Yierpan et al.<sup>20</sup>. Spinel grains were visible in some peridotites after digestion. However, orthopyroxene, clinopyroxene and spinel in peridotites do not contain detectable amounts of Se<sup>43</sup>, and instead, this element is considered to be mainly hosted in base metal sulfides and platinum group minerals<sup>22,43</sup>. Moreover, several studies where mantle rocks were digested with inverse *aqua regia* in a high-pressure asher (HPA-S), a procedure that ensures complete dissolution of spinel grains, have reported whole-rock Se concentrations similar to those obtained by HF-HNO<sub>3</sub> digestion<sup>5,20,44</sup>. However, in order to evaluate the possible effects of incomplete dissolution

of spinel in the Se isotope composition of peridotites, independent digestions in two peridotite samples (FONB-93 and DR33) were carried out with an Anton Paar™ HPA-S. For this, 1 g of sample powder together with adequate amounts of Se double spike were digested with 7.5 ml of inverse *aqua regia* (14.5 M HNO<sub>3</sub> and 10.5 M HCl, 3:1 molar ratio) in quartz glass vessels at 220°C and 100 bar for 16 h. After digestion, samples were dried down at 65°C and were subsequently treated as those digested with HF-HNO<sub>3</sub> to ensure complete digestion and desilicification. Se was separated from the sample matrix using Eichrom AG1-X8 (100-200 mesh) and AG 50W-X8 (100-200 mesh) anion and cation exchange resins, respectively, following the protocol described in Yierpan et al.<sup>20</sup>.

After separation, samples were dissolved in 1 ml 2M HCl for analyses on a ThermoFisher Scientific Neptune Plus™ MC-ICP-MS coupled with a CETAC HGX-200 hydride generator (HG). Se concentration and isotope composition were measured simultaneously using the operating conditions, data acquisition and reduction procedures described in detail in Kurzawa, et al.<sup>21</sup>. Measurements were performed in low-resolution mode, with a sample uptake rate of 0.181 mL min<sup>-1</sup>. Each analysis included 40 cycles with an integration time of 4.194 s. An analytical sequence generally consisted of the measurement of a double spike NIST SRM 3149 reference standard before and after each sample, and a double spike MH-495 reference standard analysed at the beginning, the end and in the middle of the sequence. Standard solutions, and when possible samples, were prepared to have matched concentrations of ~30 ng mL<sup>-1</sup>, and under these conditions, the typical sensitivity of the instrument was ~ 900 mV on <sup>82</sup>Se using a 10<sup>11</sup> Ω amplifier. Backgrounds were measured before each sample (and standard) analysis using pure 2M HCl and were used for on-peak zero corrections.

The long-term analytical reproducibility of Se isotope measurements is 0.07‰ based on repeated analyses of the inter-laboratory standard MH-495. These analyses were done for 30 ng mL<sup>-1</sup> Se solutions and include those previously reported by Yierpan, et al.<sup>20</sup> and those performed during this study, and together they yield an average  $\delta^{82/76}\text{Se}$  value of  $-3.25 \pm 0.07\text{‰}$  (2 s.d., n = 101, Supplementary Table 3). This is in agreement with a previously reported value of  $-3.27 \pm 0.13\text{‰}$  (2 s.d., n = 10) on 15 ng mL<sup>-1</sup> Se solutions<sup>21</sup> and is within the range of literature data<sup>42,45,46</sup>. In addition, the analytical reproducibility of Se isotope measurements in peridotites was evaluated by repeated analyses of samples FONB 93 (n=5) and TUR7 (n=6), which yield a 2 s.d. of 0.10‰ (Supplementary table 2). In terms of accuracy, our average  $\delta^{82/76}\text{Se}$  of the US Geological Survey reference material BHVO-2 ( $0.15 \pm 0.10\text{‰}$ , n=4) agrees well with data reported by Yierpan, et al.<sup>20</sup> using an HF-HNO<sub>3</sub> ( $0.18 \pm 0.10\text{‰}$ ) or an HPA-S digestion ( $0.22 \pm 0.10\text{‰}$  with ~75% Se extraction). Further discussion of our reproducibility and accuracy of measurements is given in the Supplementary Information.

Each sample was individually digested and analysed 2-6 times in different analytical sessions. Particular care was taken with very depleted samples, such as harzburgite 64-3, whose digestions (up to 6) had to be combined into one before being analysed to ensure the minimum amount of Se required for precise isotope measurements (~5 ng)<sup>21</sup>. Our peridotite dataset is thus composed of 51 digestions and 32 measurements over different analytical sessions. Generally, ~30 ng of Se were analysed for fertile lherzolites, whereas for depleted

peridotites, the amount of Se analysed range between 7 to 30 ng depending on their concentrations (Supplementary Table 2). Prior to each analytical session, samples were checked for possible arbitrarily remaining germanium (Ge) that would contribute interferences. Usually, Ge signals were lower than background levels. However, if higher, 1 ml 10.5M HCl was added to the sample and subsequently dried down at 90°C<sup>20</sup>. This procedure allows for the complete elimination of Ge and, although it results in minor Se losses for rock matrices (~10-30% in the case of peridotites), any associated isotopic fractionation is corrected by the use of the double spike technique<sup>21</sup>. Other possible polyatomic interferences on measured Se isotope masses were suppressed by admixing methane throughout the entire measurement session, which also allowed for the enhancement of the Se signal<sup>21</sup>. The  $\delta^{82/76}\text{Se}$  value of each sample (and MH-495 standard), obtained after double spike deconvolution, was normalized by the average  $\delta^{82/76}\text{Se}$  of the NIST SRM 3149 standard measured immediately before and after the sample. As published Se concentrations exist for most of the samples analysed in this study<sup>5,16,22,44,47</sup> (Supplementary table 2), an almost exact spike-to-sample ratio was adjusted without pre-concentration measurements. In the few cases where Se concentrations were unknown, samples were first analysed with an iCap-Qc ICP-MS, as described below.

A ThermoFisher Scientific iCAP-Qc ICP-MS coupled with an ESI hydrideICP HG system was used for pre-concentration Se measurements. The analytical procedure has been described in detail in Yierpan, et al. <sup>20</sup> and Kurzawa et al. <sup>21</sup>. Setting parameters were tuned daily by using ~0.5 ng g<sup>-1</sup> Se of unspiked NIST SRM 3149 standard solution, and measurements were performed in the Icap-Qc STD mode for highest sensitivity. The <sup>77</sup>Se and <sup>78</sup>Se isotopes were monitored with a dwell time of 0.03s. Samples were prepared to have matched concentrations with the standard, and under typical operating conditions, the standard solution yielded intensities of ~ 30.000 cps on <sup>78</sup>Se. Each analytical session included four standard solutions, three measured at the beginning and one at the end of the session. Backgrounds were measured before each sample and standard analysis using pure 2M HCl and were then subtracted from their analysed peak intensities, followed by correction of instrumental mass bias using the natural <sup>77</sup>Se/<sup>78</sup>Se ratio. Counts for Se were based on ~400 measurements per sample after signal stabilization and thereafter converted to concentrations (ng g<sup>-1</sup>).

Total analytical blanks, which were processed using the same procedure as outlined above for the samples, were indistinguishable from background intensities (equivalent to ~0.05 ng mL<sup>-1</sup>Se<sup>17</sup>) during analysis, and the recovery yield of Se, including sample dissolution, ion exchange chemistry and hydride generation efficiency, ranged between ~60-95%. Regarding the use of different digestion techniques, the Se concentrations and  $\delta^{82/76}\text{Se}$  values of samples FONB-93 and DR33 digested by HPA-S are indistinguishable, within error, to those obtained using HF-HNO<sub>3</sub> digestion, and thus they are considered in the average concentrations and isotopic values of each sample (Supplementary table 2). The Se concentration and isotopic signature of peridotites are independent of the digestion technique used here, which confirms earlier observations on the Se isotope composition of basalts<sup>20</sup>.

## Supplementary Material

Refer to Web version on PubMed Central for supplementary material.

## Acknowledgements

This work was supported by the ERC Starting Grant 636808 (O2RIGIN) granted to S.K. We thank T. Kurzawa and E. Reitter for laboratory assistance.

## References

1. Marty B. The origins and concentrations of water, carbon, nitrogen and noble gases on Earth. *Earth and Planetary Science Letters*. 2012; 313–314:56–66.
2. Fischer-Gödde M, Kleine T. Ruthenium isotopic evidence for an inner Solar System origin of the late veneer. *Nature*. 2017; 541:525. [PubMed: 28128236]
3. Morbidelli A, et al. Source regions and timescales for the delivery of water to the Earth. *Meteoritics & Planetary Science*. 2000; 35:1309–1320.
4. Albarède F. Volatile accretion history of the terrestrial planets and dynamic implications. *Nature*. 2009; 461:1227. [PubMed: 19865163]
5. Wang Z, Becker H. Ratios of S, Se and Te in the silicate Earth require a volatile-rich late veneer. *Nature*. 2013; 499:328–331. [PubMed: 23868263]
6. McDonough WF, Sun Ss. The composition of the Earth. *Chemical Geology*. 1995; 120:223–253.
7. Chou C-L. Fractionation of siderophile elements in the Earth's upper mantle. *Lunar and Planetary Science Conference Proceedings*. 1978; IX:219–230.
8. Walker RJ. Highly siderophile elements in the Earth, Moon and Mars: Update and implications for planetary accretion and differentiation. *Chemie der Erde - Geochemistry*. 2009; 69:101–125.
9. Rose-Weston L, Brenan JM, Fei Y, Secco RA, Frost DJ. Effect of pressure, temperature, and oxygen fugacity on the metal-silicate partitioning of Te, Se, and S: Implications for earth differentiation. *Geochimica et Cosmochimica Acta*. 2009; 73:4598–4615.
10. Mann U, Frost DJ, Rubie DC, Becker H, Audétat A. Partitioning of Ru, Rh, Pd, Re, Ir and Pt between liquid metal and silicate at high pressures and high temperatures - Implications for the origin of highly siderophile element concentrations in the Earth's mantle. *Geochimica et Cosmochimica Acta*. 2012; 84:593–613.
11. Brenan JM, McDonough WF. Core formation and metal-silicate fractionation of osmium and iridium from gold. *Nature Geoscience*. 2009; 2:798.
12. Walker RJ, et al. Comparative 187Re-187Os systematics of chondrites: Implications regarding early solar system processes. *Geochimica et Cosmochimica Acta*. 2002; 66:4187–4201.
13. Meisel T, Walker RJ, Irving AJ, Lorand J-P. Osmium isotopic compositions of mantle xenoliths: a global perspective. *Geochimica et Cosmochimica Acta*. 2001; 65:1311–1323.
14. Warren PH. Stable-isotopic anomalies and the accretionary assemblage of the Earth and Mars: A subordinate role for carbonaceous chondrites. *Earth and Planetary Science Letters*. 2011; 311:93–100.
15. Kruijer TS, Burkhardt C, Budde G, Kleine T. Age of Jupiter inferred from the distinct genetics and formation times of meteorites. *Proceedings of the National Academy of Sciences*. 2017; 114:6712–6716.
16. König S, Lorand J-P, Luguet A, Pearson DG. A non-primitive origin of near-chondritic S–Se–Te ratios in mantle peridotites; implications for the Earth's late accretionary history. *Earth and Planetary Science Letters*. 2014; 385:110–121.
17. Yierpan A, König S, Labidi J, Schoenberg R. Selenium isotope and S-Se-Te elemental systematics along the Pacific-Antarctic ridge: Role of mantle processes. *Geochimica et Cosmochimica Acta*. 2019; 249:199–224.
18. Alexander CMOD, et al. The Provenances of Asteroids, and Their Contributions to the Volatile Inventories of the Terrestrial Planets. *Science*. 2012; 337:721–723. [PubMed: 22798405]



19. Labidi J, König S, Kurzawa T, Yierpan A, Schoenberg R. The selenium isotopic variations in chondrites are mass-dependent; Implications for sulfide formation in the early solar system. *Earth and Planetary Science Letters*. 2018; 481:212–222.
20. Yierpan A, et al. Chemical Sample Processing for Combined Selenium Isotope and Selenium-Tellurium Elemental Investigation of the Earth's Igneous Reservoirs. *Geochemistry, Geophysics, Geosystems*. 2018; 19:516–533.
21. Kurzawa T, König S, Labidi J, Yierpan A, Schoenberg R. A method for Se isotope analysis of low ng-level geological samples via double spike and hydride generation MC-ICP-MS. *Chemical Geology*. 2017; 466:219–228.
22. Lorand J-P, Alard O. Determination of selenium and tellurium concentrations in Pyrenean peridotites (Ariege, France): New insight into S/Se/Te systematics of the upper in mantle samples. *Chemical Geology*. 2010; 278:120–130.
23. Lorand J-P, Alard O. Platinum-group element abundances in the upper mantle: new constraints from in situ and whole-rock analyses of Massif Central xenoliths (France). *Geochimica et Cosmochimica Acta*. 2001; 65:2789–2806.
24. Lorand J-P, Alard O, Luguët A, Keays RR. Sulfur and selenium systematics of the subcontinental lithospheric mantle: inferences from the Massif Central xenolith suite (France). *Geochimica et Cosmochimica Acta*. 2003; 67:4137–4151.
25. Harvey J, König S, Luguët A. The effects of melt depletion and metasomatism on highly siderophile and strongly chalcophile elements: S–Se–Te–Re–PGE systematics of peridotite xenoliths from Kilbourne Hole, New Mexico. *Geochimica et Cosmochimica Acta*. 2015; 166:210–233.
26. Kurzawa T, König S, Alt JC, Yierpan A, Schoenberg R. The role of subduction recycling on the selenium isotope signature of the mantle: Constraints from Mariana arc lavas. *Chemical Geology*. 2019
27. Rouxel O, Ludden J, Carignan J, Marin L, Fouquet Y. Natural variations of Se isotopic composition determined by hydride generation multiple collector inductively coupled plasma mass spectrometry. *Geochimica et Cosmochimica Acta*. 2002; 66:3191–3199.
28. Scott, ERD, Krot, AN. *Treatise on Geochemistry*. Second Edition. Holland, Heinrich D, Turekian, Karl K, editors. Elsevier; 2014. 65–137.
29. Labidi J, Cartigny P, Moreira M. Non-chondritic sulphur isotope composition of the terrestrial mantle. *Nature*. 2013; 501:208–211. [PubMed: 24005324]
30. Suer T-A, Siebert J, Remusat L, Menguy N, Fiquet G. A sulfur-poor terrestrial core inferred from metal–silicate partitioning experiments. *Earth and Planetary Science Letters*. 2017; 469:84–97.
31. Palme, H, O'Neill, HSC. *Treatise on Geochemistry*. Second Edition. Holland, Heinrich D, Turekian, Karl K, editors. Elsevier; 2014. 1–39.
32. Righter K, Humayun M, Danielson L. Partitioning of palladium at high pressures and temperatures during core formation. *Nature Geoscience*. 2008; 1:321.
33. Fischer-Gödde M, Becker H. Osmium isotope and highly siderophile element constraints on ages and nature of meteoritic components in ancient lunar impact rocks. *Geochimica et Cosmochimica Acta*. 2012; 77:135–156.
34. Hopp T, Kleine T. Nature of late accretion to Earth inferred from mass-dependent Ru isotopic compositions of chondrites and mantle peridotites. *Earth and Planetary Science Letters*. 2018; 494:50–59.
35. Creech JB, et al. Late accretion history of the terrestrial planets inferred from platinum stable isotopes. *Geochemical Perspectives Letters*. 2017; 3:94–104.
36. Creech JB, Moynier F, Bizzarro M. Tracing metal–silicate segregation and late veneer in the Earth and the ureilite parent body with palladium stable isotopes. *Geochimica et Cosmochimica Acta*. 2017; 216:28–41.
37. Fischer-Gödde, M, , et al. *Goldschmidt Abstracts*, 2018. Vol. 722. Boston: 2018.
38. Day JMD, Walker RJ, Warren JM. 186Os–187Os and highly siderophile element abundance systematics of the mantle revealed by abyssal peridotites and Os-rich alloys. *Geochimica et Cosmochimica Acta*. 2017; 200:232–254.

39. Dasgupta R, Chi H, Shimizu N, Buono AS, Walker D. Carbon solution and partitioning between metallic and silicate melts in a shallow magma ocean: Implications for the origin and distribution of terrestrial carbon. *Geochimica et Cosmochimica Acta*. 2013; 102:191–212.
40. Schönbächler M, Carlson RW, Horan MF, Mock TD, Hauri EH. Heterogeneous Accretion and the Moderately Volatile Element Budget of Earth. *Science*. 2010; 328:884–887. [PubMed: 20466929]
41. Bergin EA, Blake GA, Ciesla F, Hirschmann MM, Li J. Tracing the ingredients for a habitable earth from interstellar space through planet formation. *Proceedings of the National Academy of Sciences*. 2015; 112
42. Carignan J, Wen H. Scaling NIST SRM 3149 for Se isotope analysis and isotopic variations of natural samples. *Chemical Geology*. 2007; 242:347–350.
43. König S, Lissner M, Lorand J-P, Bragagni A, Luguët A. Mineralogical control of selenium, tellurium and highly siderophile elements in the Earth's mantle: Evidence from mineral separates of ultra-depleted mantle residues. *Chemical Geology*. 2015; 396:16–24.
44. König S, Luguët A, Lorand J-P, Wombacher F, Lissner M. Selenium and tellurium systematics of the Earth's mantle from high precision analyses of ultra-depleted orogenic peridotites. *Geochimica et Cosmochimica Acta*. 2012; 86:354–366.
45. Vollstaedt H, Mezger K, Leya I. The isotope composition of selenium in chondrites constrains the depletion mechanism of volatile elements in solar system materials. *Earth and Planetary Science Letters*. 2016; 450:372–380.
46. Zhu J-M, Johnson TM, Clark SK, Xiang-Kun Z. High precision measurement of selenium isotopic composition by hydride generation multiple collector inductively coupled plasma mass spectrometry with a  $^{74}\text{Se}$ - $^{77}\text{Se}$  double spike. *Chinese Journal of Analytical Chemistry*. 2008; 36:1385–1390.
47. Lorand J-P, Luguët A, Alard O, Bezos A, Meisel T. Abundance and distribution of platinum-group elements in orogenic lherzolites; a case study in a Fontete Rouge lherzolite (French Pyrénées). *Chemical Geology*. 2008; 248:174–194.

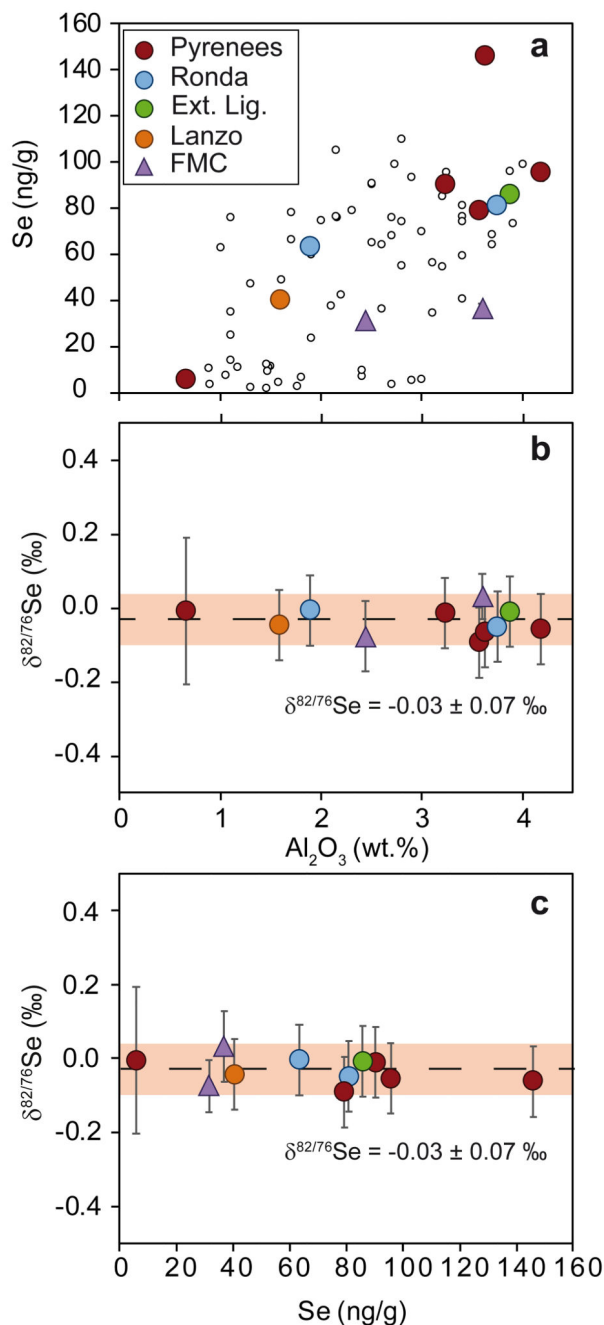


**Figure 1. Se and Al<sub>2</sub>O<sub>3</sub> contents and Se isotope data of mantle peridotites.**

(a) Se vs. Al<sub>2</sub>O<sub>3</sub>, and  $\delta^{82/76}\text{Se}$  vs. (b) Al<sub>2</sub>O<sub>3</sub> and (c) Se of post-Archean peridotites. Circles represent orogenic and transitional peridotites and triangles mantle xenoliths. Small circles in (a) correspond to previously published peridotite data<sup>5,16</sup>. 1 s.d. uncertainties on concentrations are similar or smaller than symbol size, whereas error bars in (b) and (c) indicate 2 s.d. uncertainties of more than two combined measurements. If not available, the analytical uncertainty obtained for repeated analysis of peridotites is reported ( $\pm 0.10\%$ ,

2s.d.) (see Methods). The shaded field represents the 2 s.d. of the mean of peridotites as discussed in the text.

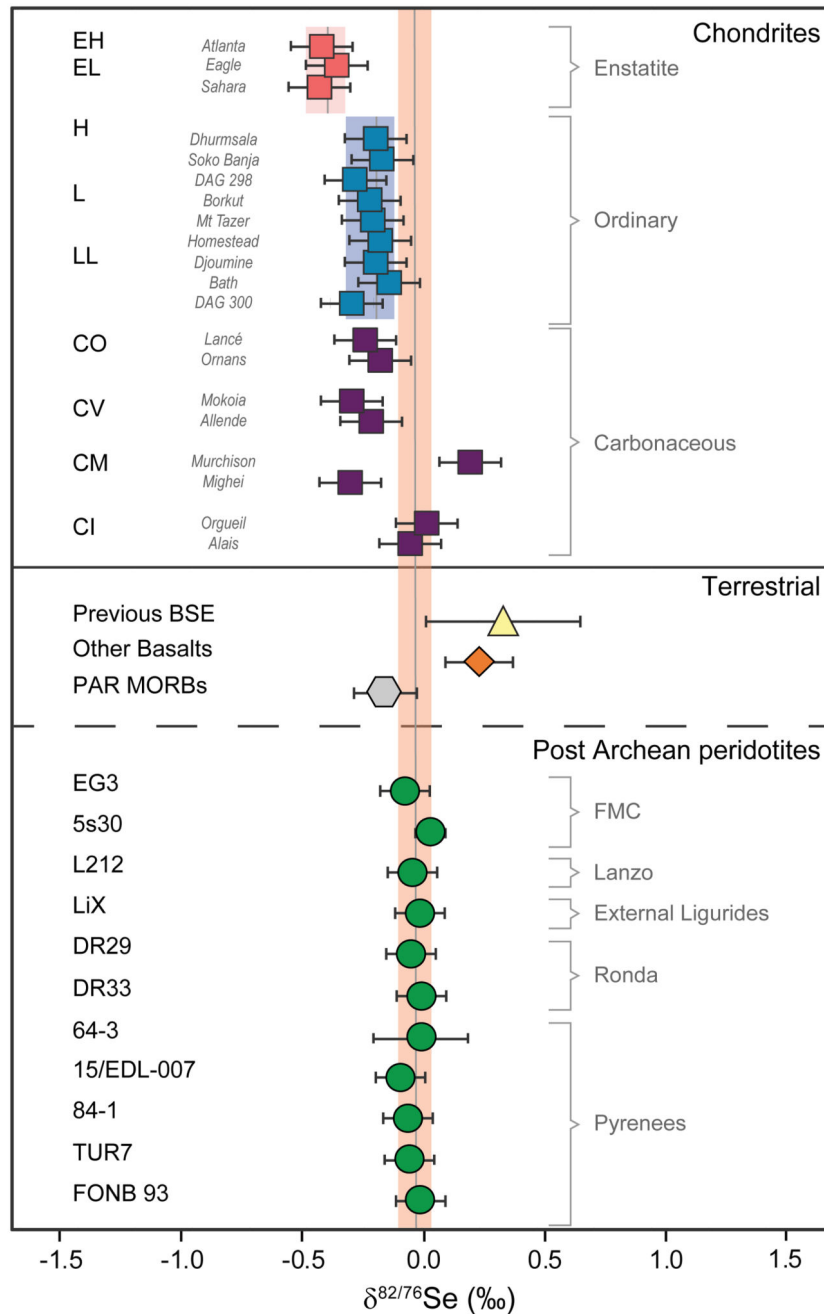


**Figure 2. Se isotope data for terrestrial and meteorite samples.**

$\delta^{82/76}\text{Se}$  values of analysed peridotites (for simplicity all as circles) together with published data for terrestrial melts, including basalts from a variety of geodynamic settings (diamond shape)<sup>20</sup>, and MORBs from the Pacific-Antarctic Ridge (PAR)<sup>17</sup>. Also shown are published data for the BSE<sup>27</sup> (2 s.d. analytical precision; average based on iron meteorites and igneous reference materials) and meteorites<sup>19</sup>. 2 s.d. analytical precision for individual chondrites is 0.13‰ and weathered chondrites are not shown, as they are associated with isotopic fractionation<sup>19</sup>. Literature data<sup>27</sup> are converted to  $\delta^{82/76}\text{Se}$  following <sup>42</sup>. Error bars for

peridotites indicate 2 s.d. uncertainties of more than two combined measurements. If not available, the analytical uncertainty obtained for repeated analyses of peridotites is reported ( $\pm 0.10\%$ , 2s.d.) (see Methods). Shaded bars indicate the mean  $\delta^{82/76}\text{Se}$  values of the BSE, and of enstatite and ordinary chondrites<sup>19</sup>,  $\pm 2$  s.d.